Rizov, *Cogent Engineering* (2015), 2: 993528
http://dx.doi.org/10.1080/23311916.2014.993528

cogent engineering

MATERIALS ENGINEERING | RESEARCH ARTICLE

Mixed-mode I/III fracture study of sandwich beams

V. Rizov[1*]

Received: 08 June 2014
Accepted: 27 November 2014
Published: 20 January 2015

*Corresponding author: V. Rizov, Department of Technical Mechanics, University of Architecture, Civil Engineering and Geodesy, 1 Chr. Smirnensky Blvd., 1046 Sofia, Bulgaria
E-mail: v_rizov_fhe@uacg.bg

Reviewing editor:
Eileen Harkin-Jones, Queen's University, UK

Additional information is available at the end of the article

Abstract: The capacity of prestressed split-cantilever beam (SCB) for investigation of mixed-mode I/III fracture in foam core sandwich constructions was evaluated theoretically. The fracture was studied in terms of the strain energy release rate. In this relation, a three-dimensional finite-element model was developed. The strain energy release rate mode components were analyzed by the virtual crack closure technique. The analysis revealed that the mode I and the mode III components have maximum at the center of the crack front and gradually decrease toward the edges. Different mixed-mode ratios were generated by varying the mutual transverse displacement at the end of the sandwich SCB crack arms (in this way, the use of steel rollers with different diameters for prestressing the SCB to provide the mode-I part of the loading was modeled). The effect of the sandwich core material on the mixed-mode I/III fracture was investigated. For this purpose, three sandwich SCB configurations with different rigid cellular foams used for core material were simulated. It was found that the strain energy release rate decreases when the foam density increases. Therefore, the mixed-mode I/III fracture performance of the sandwich beams can be improved by using foams with higher density for core material.

Subjects: Technology; Materials Science; Composites; Polymers & Plastics

Keywords: linear-elastic fracture mechanics; foam core composite sandwich beams; mixed-mode I/III crack loading; strain energy release rate

ABOUT THE AUTHOR

The key research activities of Prof. Rizov are in the field of fracture behavior of fiber-reinforced polymer composites, fracture in foam core sandwich structures, non-linear mechanical behavior of foam core sandwiches subjected to localized loads, and elastic-plastic behavior of structural materials. His research includes also experimental characterization, finite-element modelling, and closed form analytical solutions. He has published more than 120 scientific papers.

PUBLIC INTEREST STATEMENT

A theoretical study of the mixed-mode I/III fracture in foam core sandwich SCB was performed. The study was motivated by the fact that mixed-mode I/III fracture in sandwich beams has received less attention in the literature. The basic idea of the study was that mixed-mode I/III crack-loading conditions can be generated using a prestressed SCB. The prestressing was performed by inserting a steel roller between the crack arms (in this way, the mode I component was induced). The mode III component was induced by applying a scissor-like load on the crack arms. Three-dimensional finite-element simulations were conducted. The influence of the foam core on the mixed-mode I/III fracture was studied. It was found that the strain energy release rate decreases, when the foam core density increases. Thus, the use of foam with higher density can be recommended as a means for improving the mixed-mode I/III fracture performance of sandwich beams.

1. Introduction

Foam core composite sandwich structures are widely used in modern loading–bearing applications and are attracting increasing attention from engineers and researchers (Akil Hazizan & Cantwell, 2002; Avilés & Carlsson, 2008; Gibson & Ashby, 1997; Hilyard & Cunningham, 1994; Nemes & Simmonds, 1992; Soden, 1996; Steeves & Fleck, 2000). The sandwich structures can offer high strength and stiffness in conjunction with weight reduction, which is their main advantage over the traditional structural materials.

The fracture behavior in many cases is critical for the load-bearing capacity of sandwich structures. Thus, much research efforts have been given to the problem of fracture in sandwich structures and their constituents (Farshad & Flüeler, 1998; Goswami & Becker, 2001; Hernández-Pérez, Avilés, & Carlsson, 2013; Marsavina & Sadowski, 2008; Prasad & Carlsson, 1994a, 1994b; Quispitupa, Berggreen, & Carlsson, 2009; Ramantani, de Moura, Campilho, & Marques, 2010; Shen, Cantwell, & Li, 2014; Sun, Yang, & Jia, 2014; Theotokoglou & Theotokoglou, 2013). Goswami and Becker simulated a delamination crack along the face sheet/core interface in a sandwich structure using a two-dimensional finite-element model (Goswami & Becker, 2001). Prasad and Carlsson used modified double cantilever beam and shear fracture sandwich specimens for studying face/core debond fracture and crack kinking (Prasad & Carlsson, 1994a, 1994b). Farshad and Flüeler characterized mode III fracture toughness of rigid foams using as anti-clastic plate bending test method (Farshad & Flüeler, 1998). The fracture specimens were analyzed by finite-element method models. Dynamic fracture in polyurethane foam is investigated by using a three-point bend specimen in Marsavina and Sadowski (2008). Fracture behavior of foam core sandwich beams is analyzed by Quispitupa et al. (2009). Mode I fracture of sandwich structures is studied in Ramantani et al. (2010). Analysis of fractured lightweight sandwich beams is performed by Theotokoglou and Theotokoglou (2013). Mode III fracture of foam core sandwich panels with steel face sheets is investigated in Hernández-Pérez et al. (2013). The interface fracture toughness of a sandwich structure is studied by Shen et al. (2014). Face/core fracture in composite sandwich is investigated by Sun et al. (2014).

However, mixed-mode I/III fracture behavior of sandwich beams has received less attention in the literature. Therefore, the main purpose of the present paper was to perform a theoretical study of mixed-mode I/III fracture in foam core composite sandwich beams using a prestressed Split Cantilever Beam (SCB).

2. Analysis of strain energy release rate in the prestressed sandwich SCB

The sandwich SCB under consideration in the present paper is illustrated in Figure 1. The sandwich beam consists of 2.5 mm thick polymer composite face sheets adhesively bonded to a 50 mm thick lightweight rigid cellular foam core. The overall dimensions of the sandwich SCB are 60 mm × 55 mm × 500 mm. In the mid-plane of the sandwich beam, there is a longitudinal crack, a, with length of 300 mm.

In order to generate mixed-mode I/III crack-loading conditions in the sandwich SCB, the concept developed by Szekrényes (2009) was applied. The basic idea of this concept was that the SCB should be prestressed by pressing a steel roller between the crack arms. In this way, the mode I component of the crack loading was induced. The mode III component was generated by applying two loads, F_1 and F_2, to each crack arm. For this purpose, a special loading rig consisting of two identical steel plates was used. The concept of prestressed SCB specimen was developed originally for the investigation of mixed-mode I/III interlaminar fracture behavior of unidirectional glass-fiber-reinforced polyester material in Szekrényes (2009).

For the problem under consideration (Figure 1), the loads F_1 and F_2 were determined by analyzing the equilibrium of one steel plate of the rig (Figure 2). The result was $F_1 = 0.857$ F and $F_2 = 1.857$ F [this result was obtained by using the moment equilibrium equations for points B and C (Figure 2)]. The loads, F_1 and F_2, were applied to the crack arms of the prestressed sandwich SCB through loading noses, B and C, respectively (Figure 2). It should be mentioned that the application point, A, of the

Figure 1. Prestressed sandwich SCB geometry and loading.

Note: The mode-I part of the loading is provided by inserting a steel roller between the crack arms.

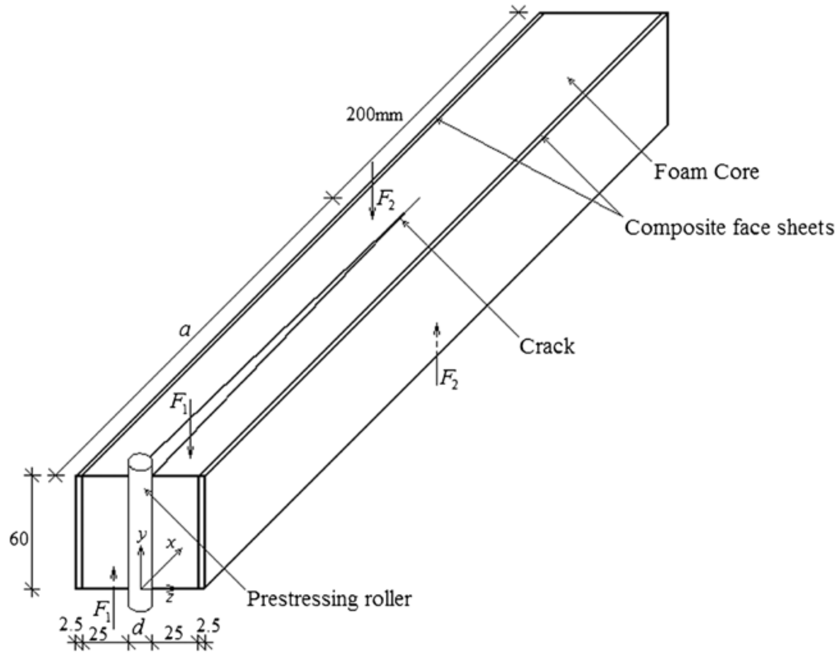

Figure 2. Loading of the sandwich SCB applied by one steel plate of the rig.

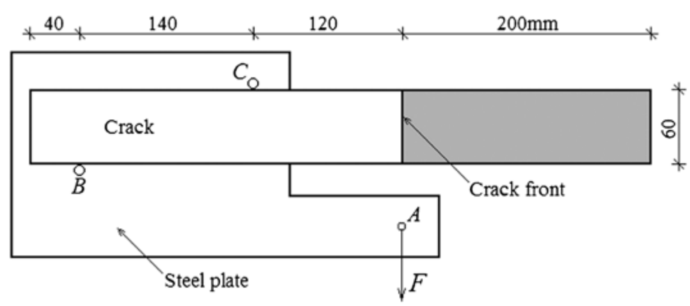

external load, F, was chosen such that the load line was collinear with the crack front. In this way, the bending moment in the arms of the sandwich SCB at the crack front was reduced to zero. This was done in order to minimize the undesired mode II component of the crack loading as suggested by Sharif, Kortschot, and Martin (1995) who used the SCB specimen for investigation of pure mode III delamination fracture behavior of carbon-fiber-reinforced epoxy laminates.

End view of the prestressed foam core composite sandwich SCB and the plates of the rig are depicted in Figure 3.

A three-dimensional finite-element model was developed in order to simulate the mechanical response of the prestressed foam core composite sandwich SCB configuration and to evaluate the strain energy release rate. The modeling was performed using the ANSYS finite-element computer code. The model was based on the geometry and the dimensions shown in Figure 1. The model was meshed using three-dimensional continuum brick finite-element SOLID45. This element is defined by eight nodes (one at each vertex) having three degrees of freedom per node (translation in the nodal x, y, and z directions). A total of 4,920 elements were used. The mesh was refined in the crack front area to allow for a more accurate analysis of the strain energy release rate mode components distribution. It has to be pointed out that before carrying-out further simulations, a mesh sensitivity study was performed in order to ensure that the mesh was fine enough to give reliable results. The mesh used in the modeling of the prestressed sandwich SCB configuration is illustrated in Figure 4.

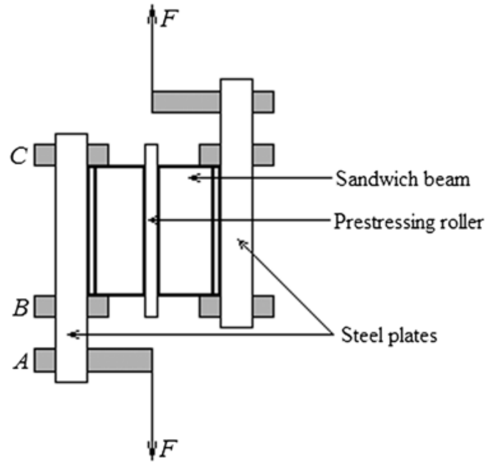

Figure 3. End view of the prestressed sandwich SCB and the rig.

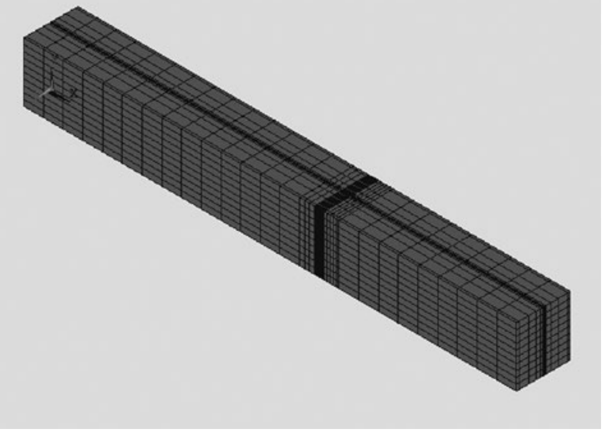

Figure 4. Finite-element mesh for modeling of the sandwich SCB.

The elastic properties of the composite face sheets used in the finite-element simulations of the sandwich SCB configuration are reported in Table 1. The influence was studied of the core material on the mixed-mode I/III fracture behavior of the sandwich beam. For this purpose, it was presumed that the core was made of three different rigid cellular foams (Divinycell H45, Divinycell H100, and Divinycell HCP100), i.e. three sandwich beam configurations were considered. It should be mentioned that these foams are frequently used as core material in sandwich constructions. Divinycell polyvinylchloride (PVC) foams are fully cross-linked rigid foams with closed-cell structure. The manufacturing process of these foams basically consists in mixing the chemical polymer components together and carrying out the thermal expansion of the polymer mass in hot water. In the finite-element modeling, the foam core was regarded as a linear-elastic material (the corresponding elastic properties are reported in Table 2).

Table 1. Elastic properties of the composite face sheets used in the simulations of the prestressed sandwich SCB. The subscripts refer to the principal material axes, *x*, *y*, and *z*, defined in Figure 1

E_{xx} (GPa)	E_{yy} (GPa)	E_{zz} (GPa)	G_{xy} (GPa)	G_{yz} (GPa)	G_{zx} (GPa)	ν_{xy}	ν_{yz}	ν_{zx}
40.700	10.269	10.269	4.200	3.980	4.200	0.29	0.27	0.29

Table 2. Elastic properties and densities of the rigid cellular foams used in the finite-element modeling of the prestressed foam core sandwich SCB

	E (GPa)	ν	γ (kg/m^3)
Divinycell H45	0.042	0.295	45
Divinycell H100	0.105	0.310	100
Divinycell HCP100	0.340	0.300	400

The finite-element model was loaded by vertical forces, F_1 and F_2, applied at the crack arms according to the scheme depicted in Figure 1. The prestressing was modeled as a prescribed horizontal displacement along the z-axis (refer to the coordinate system in Figure 1) applied at the end of the sandwich SCB crack arm (the displacement value was equal to half of the diameter of steel roller used to prestress the beam). In this way, the mode-I part of the crack loading was provided.

The sandwich SCB free end, x = 500 mm (Figure 1), was fixed in order to prevent rigid body movement of the model. The deformed state of the model is reported in Figure 5.

The main aim of the finite-element modeling was to compute the strain energy release rate mode components for the three sandwich SCB configurations considered at different values of the diameter of steel roller. For this purpose, the virtual crack closure technique was applied. This is a commonly used technique which is based on linear-elastic fracture mechanics (Rybicki & Kanninen, 1977; Shivakumar & Newman, 1988; Suemasu, Kumagai, & Gozu, 1998; Szekrényes & Uj, 2006; Whitcomb, 1991). The virtual crack closure technique allows the strain energy release rate component associated with the three basic modes of crack growth to be calculated separately. The advantage of this technique is that it requires only one analysis by the finite-element model for the actual crack length. The virtual crack closure technique uses the nodal forces in the crack front and the nodal displacements behind the crack front. A three-dimensional scheme of the near crack front region with nodal notations is depicted in Figure 6. The virtual crack closure technique assumes that the work done to close the crack by one element length is equivalent to the strain energy released when the crack grows by one element. Thus, the strain energy release rate mode components, G_{I}, G_{II}, and G_{III}, at point i in the crack front can be calculated using the following formulae:

$$G_{\mathrm{I}} = \frac{1}{2\Delta a \Delta h} Z_i (w_j - w_k) \tag{1}$$

Figure 5. Deformed state of the model (the displacements are exaggerated for clarity).

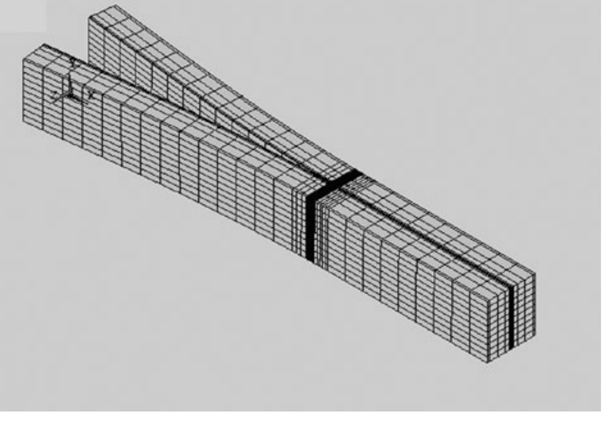

Figure 6. Schematic of the finite-element mesh in the vicinity of the node *i* at the crack front with nodal notations.

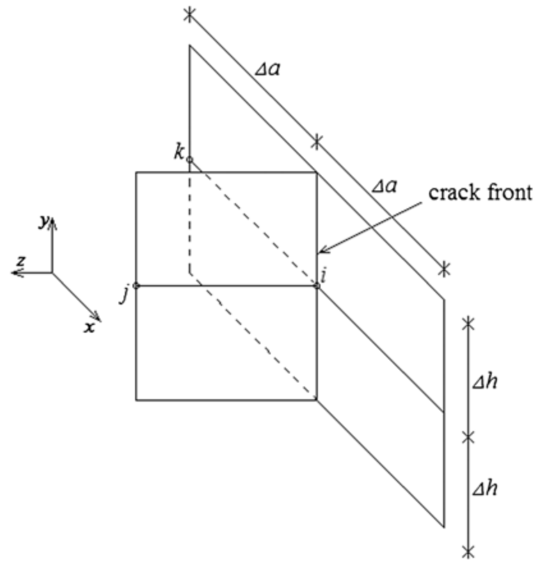

$$G_{\mathrm{II}} = \frac{1}{2\Delta a \Delta h} X_i (u_j - u_k) \tag{2}$$

$$G_{\mathrm{III}} = \frac{1}{2\Delta a \Delta h} Y_i (v_j - v_k) \tag{3}$$

where X, Y, and Z are the nodal force components; u, v, and w are the nodal displacement components in x, y, and z directions, respectively. The subscripts in Equations 1–3 denote the corresponding nodes in Figure 6. The distribution of the strain energy release rate mode components on the sandwich SCB height was analyzed by applying Equations 1–3 at each node along the crack front. It should be mentioned that a sensitivity study was performed in order to evaluate the effect of the element length, Δa, on the strain energy release rate (Figure 6). For this purpose, simulations were carried-out using three different element lengths (Δa = 2, 1, and 0.5 mm). The average value of the total strain energy release rate along the crack front was calculated using formulae 7–10 for these three element lengths. The results obtained are reported in Table 3. It can be seen that the average value of the total strain energy release rate for Δa = 1 mm and Δa = 0.5 mm does not change (Table 3). Thus, it was decided to use Δa = 1 mm in further simulations.

Although the virtual crack closure technique is frequently used, because it requires only one analysis by the finite-element model and it is an indirect method for computation of the strain energy release rate. Therefore, the results obtained by Equations 1–3 were verified by the crack closure technique, which is a direct method of computing the strain energy release rate based on the principles of linear-elastic fracture mechanics. The application of the crack closure technique requires two analyses by the finite-element model.

Table 3. Average value of the normalized total strain energy release rate along the crack front, G^{aN}, at different element length, Δa

Δa (mm)	G^{aN}
2.0	0.0194
1.0	0.0208
0.5	0.0208

In the first analysis, which is carried-out for the actual crack length, i.e. just prior to crack growth, the nodal forces at the crack front are computed. The crack growth is simulated in the second analysis by releasing the crack front nodes. The second analysis provides the corresponding nodal displacements needed to compute the strain energy release rate mode components. The crack closure technique assumes that the nodal forces determined in the first analysis are the forces required to close the crack. The work done during the process of crack closure can be calculated by multiplying one half the nodal forces with the corresponding nodal displacements. The strain energy release rate mode components in node *i* in the crack front (Figure 6) can be computed using the expressions

$$G_{\mathrm{I}} = \frac{1}{2\Delta a \Delta h} Z_i \delta w_i \tag{4}$$

$$G_{\mathrm{II}} = \frac{1}{2\Delta a \Delta h} X_i \delta u_i \tag{5}$$

$$G_{\mathrm{III}} = \frac{1}{2\Delta a \Delta h} Y_i \delta v_i \tag{6}$$

where δu_i, δv_i, and δw_i are the differences in the nodal displacement components; X_i, Y_i, and Z_i are the nodal force components determined in the first calculation by the finite-element model of the sandwich SCB.

The discrepancy between the strain energy release rate obtained by the virtual crack closure technique and the crack closure technique was within 2%, which was an indication for the accuracy of the computations.

The average values of strain energy release rate mode components along the crack front were calculated as

$$G_{\mathrm{I}}^{a} = \frac{1}{h} \int_0^h G_{\mathrm{I}}(y) dy \tag{7}$$

$$G_{\mathrm{II}}^{a} = \frac{1}{h} \int_0^h G_{\mathrm{II}}(y) dy \tag{8}$$

$$G_{\mathrm{III}}^{a} = \frac{1}{h} \int_0^h G_{\mathrm{III}}(y) dy \tag{9}$$

where $G_{\mathrm{I}}(y)$, $G_{\mathrm{II}}(y)$, and $G_{\mathrm{III}}(y)$ are the strain energy release rate mode components distribution along the crack front obtained by Equations 1–3, and h is the crack front length, i.e. the sandwich SCB height.

The average value of the total strain energy release rate along the crack front was obtained as

$$G^{a} = G_{\mathrm{I}}^{a} + G_{\mathrm{II}}^{a} + G_{\mathrm{III}}^{a} \tag{10}$$

The influence was considered of the diameter value of the steel roller on the character of the fracture behavior. In order to evaluate this influence, the strain energy release rate was analyzed at three diameter values (d = 45, 60, and 75 mm). The distributions of the normalized strain energy release rate mode components along the crack front at the three roller diameter values are reported in Figure 7 (the strain energy release rate mode components were normalized using the formula $G_i^N = G_i h/F$, where i = I, II, and III). Only half of the crack front is shown due to the symmetric character of the distribution with respect to the crack front center. It can be observed in Figure 7 that the distribution of the mode I and the mode III components is characterized by maximum at the crack front center and a gradual decrease toward the edges of the sandwich SCB cross-section. As can be seen (Figure 7) beside mode I and mode III components, there is also mode II component, which, however, is relatively small. Since the strain energy release rate distribution was non-uniform, the influence of the roller diameter on the fracture behavior was evaluated by analyzing the mixed-mode ratios of the average values of the strain energy release rate mode components along the crack front, G_{I}^a/G^a, G_{II}^a/G^a, and G_{III}^a/G^a. The average values were calculated by formulae 7–10. The integrals were solved numerically. The mixed-mode ratios obtained are reported in Table 4. It can be seen that the relative amount of mode I component increases when the roller diameter increases (Table 4). The relative amounts of mode II and mode III components decrease with an increase in the roller diameter. Thus, by varying the roller diameter, broad mixed-mode ratios ranges can be achieved. The data in Table 4 indicate that the relative amount of mode II component is small, i.e. the prestressed sandwich SCB configuration considered (Figure 1) can be used to investigate the mixed-mode I/III fracture in sandwich structures.

Figure 7. Normalized strain energy release rate mode components distribution along the crack front in the sandwich SCB prestressed by a steel roller with a diameter of (a) 45 mm, (b) 60 mm, and (c) 75 mm.

Notes: The horizontal axis is defined such that *y/h* = 0.0 is at the lower edge of the sandwich beam cross-section; thus, *y/h* = 0.5 is at the crack front center (here *h* is the height of the sandwich beam cross-section). The sandwich core is made by Divinycell H45.

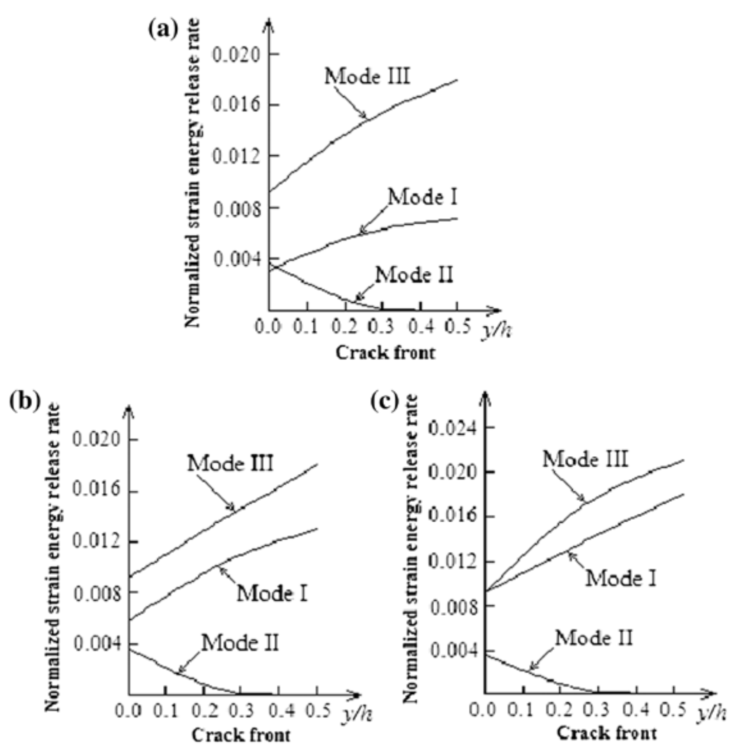

Table 4. Mixed-mode ratios of the average values of the strain energy release rate mode components along the crack front (G_{I}^a/G^a, G_{II}^a/G^a, and G_{III}^a/G^a) in the foam core sandwich SCB prestressed by a steel roller with diameter *d* (refer to Figure 1)

Steel roller diameter, *d* (mm)	G_{I}^a/G^a	G_{II}^a/G^a	G_{III}^a/G^a
45	0.175	0.067	0.758
60	0.377	0.050	0.573
75	0.495	0.040	0.465

Note: The sandwich core is made by Divinycell H45.

The effect of the sandwich core material on the mixed-mode I/III fracture behavior was evaluated by simulating three sandwich SCB configurations with different rigid cellular foams (Divinycell H45, Divinycell H100, and Divinycell HCP100) used for core material. The strain energy release rate was analyzed by the virtual crack closure technique via Equations 1–3. The results yielded by the analysis are presented in Figure 8. The diagrams indicate that the strain energy release rate decreases, when the foam modulus of elasticity increases (Figure 8). It can be seen in Table 2 that the foam modulus of elasticity increases with an increase in the foam density. Therefore, the use of rigid cellular foams with higher density can be recommended with purpose to improve the mixed-mode I/III fracture performance of foam core sandwich beams.

3. Conclusions

In the present paper, a theoretical study was performed of the mixed-mode I/III fracture in foam core composite sandwich beams using a prestressed SCB configuration. The methods of linear-elastic fracture mechanics were applied. A three-dimensional finite-element model of the prestressed sandwich SCB was developed using the ANSYS computer code. The mode-I part of the loading was simulated by applying different mutual transverse displacements at the end of the crack arms. In this way, the prestressing of the sandwich SCB, performed by inserting a steel roller between the crack arms, was modeled. The mode-III part of the loading was simulated by applying a scissor-like load to the crack arms of the prestressed sandwich SCB. The fracture behavior was studied in terms of the strain energy release rate using the finite-element model and the virtual crack closure technique. The results obtained were confirmed by the crack closure technique. The following conclusions were drawn:

(1) The analysis revealed non-uniform distribution of the strain energy release rate mode components along the crack front. Therefore, the effect of the prestressing on the fracture behavior was studied by analyzing the mixed-mode ratios of the average values of the strain energy release rate mode components along the crack front.

Figure 8. Normalized strain energy release rate mode components distribution along the crack front in the prestressed sandwich SCB with foam core made by (a) Divinycell H45, (b) Divinycell H100, and (c) Divinycell HCP100.

Notes: The horizontal axis is defined such that *y/h* = 0.0 is at the lower edge of the sandwich beam cross-section; thus, *y/h* = 0.5 is at the crack front center (here *h* is the height of the sandwich beam cross-section). The sandwich SCB is prestressed by a steel roller with a diameter of 60 mm.

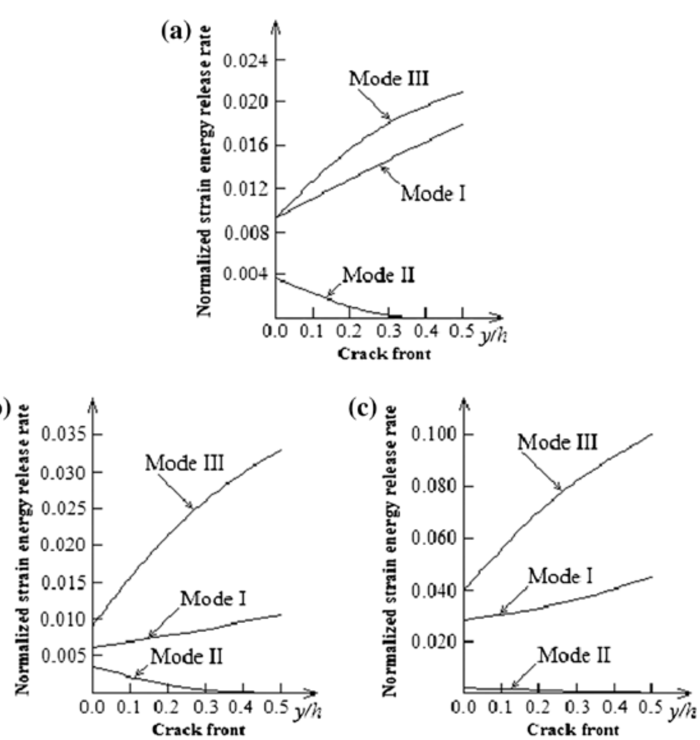

(2) It was found that the relative amount of mode I component increases with an increase in the roller diameter. The relative amounts of mode II and mode III components decrease when the roller diameter increased.

(3) The results obtained indicate that the prestressed sandwich SCB configuration can be used to investigate the mixed-mode I/III fracture over broad mixed-mode ratios ranges.

(4) The influence of the sandwich core material on the mixed-mode I/III fracture was studied too. For this purpose, sandwich SCB configurations with three different foam cores were simulated. It was found that the strain energy release rate decreases when the foam density increases. Thus, the fracture performance of the sandwich beams can be improved significantly by using rigid cellular foams with higher density as a core material.

Funding
The authors received no direct funding for this research.

Author details
V. Rizov[1]
E-mail: v_rizov_fhe@uacg.bg
[1] Department of Technical Mechanics, University of Architecture, Civil Engineering and Geodesy, 1 Chr. Smirnensky Blvd., 1046 Sofia, Bulgaria.

Citation information
Cite this article as: Mixed-mode I/III fracture study of sandwich beams, V. Rizov, *Cogent Engineering* (2015), 2: 993528.

References

Akil Hazizan, Md., & Cantwell, W. J. (2002). The low velocity impact response of foam-based sandwich structures. *Composites Part B: Engineering, 33*, 193–204. http://dx.doi.org/10.1016/S1359-8368(02)00009-4

Avilés, F., & Carlsson, L. A. (2008). Analysis of the sandwich DCB specimen for debond characterization. *Engineering Fracture Mechanics, 75*, 153–168. http://dx.doi.org/10.1016/j.engfracmech.2007.03.045

Farshad, M., & Flüeler, P. (1998). Investigation of mode III fracture toughness using an anti-clastic plate bending method. *Engineering Fracture Mechanics, 60*, 597–603. http://dx.doi.org/10.1016/S0013-7944(98)00020-4

Gibson, L. J., & Ashby, M. F. (1997). *Cellular solids*. Cambrige: Cambrige University Press. http://dx.doi.org/10.1017/CBO9781139878326

Goswami, S., & Becker, W. (2001). The effect of facesheet/core delamination in sandwich structures under transverse loading. *Composite Structures, 54*, 515–521. http://dx.doi.org/10.1016/S0263-8223(01)00124-6

Hernández-Pérez, A., Avilés, F., & Carlsson, L. A. (2013). Evaluation of the plate twist test to characterize mode III fracture of sandwich panels with a face/core interface crack. *Engineering Fracture Mechanics, 104*, 41–55. http://dx.doi.org/10.1016/j.engfracmech.2013.03.014

Hilyard, N. C., & Cunningham, A. (1994). *Low density cellular plastics*. London: Chapman & Hall. http://dx.doi.org/10.1007/978-94-011-1256-7

Marsavina, L., & Sadowski, T. (2008). Dynamic fracture toughness of polyurethane foam. *Polymer Testing, 27*, 941–944. http://dx.doi.org/10.1016/j.polymertesting.2008.08.006

Nemes, J. A., & Simmonds, K. E. (1992). Low-velocity impact response of foam-core sandwich composites. *Journal of Composite Materials, 26*, 500–519. http://dx.doi.org/10.1177/002199839202600403

Prasad, S., & Carlsson, L. A. (1994a). Debonding and crack kinking in foam core sandwich beams—I. Analysis of fracture specimens. *Engineering Fracture Mechanics, 47*, 813–824. http://dx.doi.org/10.1016/0013-7944(94)90061-2

Prasad, S., & Carlsson, L. A. (1994b). Debonding and crack kinking in foam core sandwich beams—II. Experimental investigation. *Engineering Fracture Mechanics, 47*, 825–841. http://dx.doi.org/10.1016/0013-7944(94)90062-0

Quispitupa, A., Berggreen, C., & Carlsson, L. A. (2009). On the analysis of a mixed mode bending sandwich specimen for debond fracture characterization. *Engineering Fracture Mechanics, 76*, 594–613. http://dx.doi.org/10.1016/j.engfracmech.2008.12.008

Ramantani, D. A., de Moura, M. F. S. F., Campilho, R. D. S. G., & Marques, A. T. (2010). Fracture characterization of sandwich structures interfaces under mode I loading. *Composites Science and Technology, 70*, 1386–1394. http://dx.doi.org/10.1016/j.compscitech.2010.04.018

Rybicki, E. F., & Kanninen, M. F. (1977). A finite element calculation of stress intensity factors by a modified crack closure integral. *Engineering Fracture Mechanics, 9*, 931–938.http://dx.doi.org/10.1016/0013-7944(77)90013-3

Sharif, F., Kortschot, M. T., & Martin, R. H. (1995). Mode III delamination using a split cantilever beam. *Composite Materials: Fatigue and Fracture,* ASTM STP, *5*, 85–99.

Shen, Y., Cantwell, W., & Li, Y. (2014). Skin-core adhesion in high performance sandwich structures. *Journal of Zhejiang University-SCIENCE A (Applied Physics & Engineering), 15*, 61–67.

Shivakumar, K. N., & Newman, J. C. (1988). A virtual crack-closure technique for calculation of stress intensity factor for cracked three-dimensional bodies. *International Journal of Fracture, 36*, 43–50.

Soden, P. D. (1996). Indentation of composite sandwich beams. *The Journal of Strain Analysis for Engineering Design, 31*, 353–360. http://dx.doi.org/10.1243/03093247V315353

Steeves, C. A., & Fleck, N. A. (2000, November 5–10). Failure modes in sandwich beams with composite face-sheets and PVC foam cores. *ASME ICEME'2000 Conference in Orlando,* ASME AERO AMD AD *62*/AMD *245*, 21–28.

Suemasu, H., Kumagai, T., & Gozu, K. (1998). Compressive behavior of multiply delaminated composite laminates part 2: Finite element analysis. *AIAA Journal, 36*, 1286–1290. http://dx.doi.org/10.2514/2.512

Sun, S., Yang, R., & Jia, Z. (2014). Finite element analyses of face/core interfacial fracture toughness of composite sandwich with reinforced chopped fibers. *Advances in Mechanical Engineering*, 7, Article ID 542135. Retrieved from http://dx.doi.org/10.1155/2014/542135

Szekrényes, A. (2009). Interlaminar fracture analysis in the G_I–G_{III} plane using prestressed transparent composite beams. *Composites Part A: Applied Science and Manufacturing, 40*, 1621–1631. http://dx.doi.org/10.1016/j.compositesa.2009.07.009

Szekrényes, A., & Uj, J. (2006). Comparison of some improved solutions for mixed-mode composite delamination coupons. *Composite Structures, 72*, 321–329. http://dx.doi.org/10.1016/j.compstruct.2005.01.002

Theotokoglou, E. E., Theotokoglou, G. E. (2013, June 16–21). New trends in the fracture of lightweight structures. In *13th International Conference on Fracture*. Beijing, China.

Whitcomb, J. D. (1991). Delamination growth in a laminate with a post-buckled edge delamination. *Journal of Composites Technology and Research, 13*, 175–178.